

pubs.acs.org/jasms Research Article

Investigating Electrosprayed Droplets Using Particle-into-Liquid Sampling for Nanoliter Electrochemical Reactions

Nathaneal A. Park, Gary L. Glish, and Jeffrey E. Dick*



Cite This: J. Am. Soc. Mass Spectrom. 2023, 34, 320-327



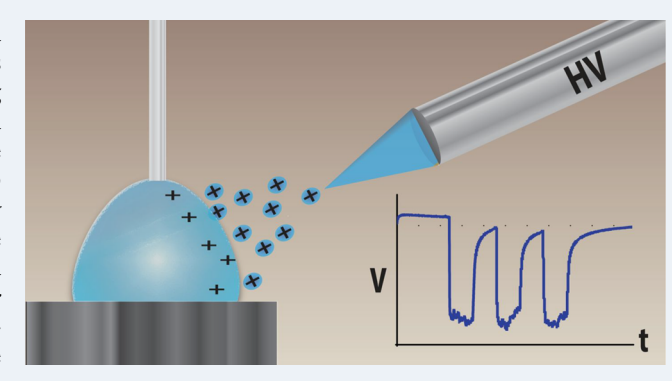
ACCESS I

III Metrics & More

Article Recommendations

s Supporting Information

ABSTRACT: Electrospray ionization (ESI) is a powerful ionization technique that can generate charged solvent droplets and bare analyte ions from sample solutions. Despite seeing extensive use in mass spectrometry due in part to the low internal energy deposited into the ions formed during ionization, some unknowns persist regarding the exact dynamics of droplet breakup and molecule behavior during spray, and research is still underway regarding how various types of molecules acquire charge during the ESI process. Previously, the authors introduced a novel aerosol measurement technique, particle-into-liquid sampling for nanoliter electrochemical reactions (PILSNER). The current work introduces a new method utilizing PILSNER for the examination of the particles generated during ESI using simple analysis techniques



with a commercially available potentiostat. This technique is applied in this work for the detection of charges on electrosprayed droplets, including the estimation of the number of charges on individual ESI droplets using a fluorescent proxy. This technique provides an additional tool for the exploration of the complex process of droplet generation and ion liberation during ESI.

■ INTRODUCTION

Electrospray ionization (ESI) has been a powerful tool for the production of gas-phase droplets and ions even before its introduction as an ion source for mass spectrometry (MS) in 1984. In ESI, analyte-containing solvent is flowed through an emitter to which a high voltage (relative to the instrument inlet in MS) is applied. The voltage causes a cone-shaped deformation of the fluid surface which can be described by the Laplace equation.² This deformation, sometimes with the aid of shear force provided by a coaxially delivered nebulizing gas, causes the liberation of droplets from the cone tip, resulting in a stream of droplets (referred to as a "Taylor cone"). This process creates highly charged solvent droplets with a large net charge and a polarity matching the net voltage applied between the electrospray emitter and the instrument inlet.² These droplets evaporate and shrink until they eventually reach the Rayleigh charge stability limit. At this limit, the repulsion between charges on the droplet surface exceeds the surface tension of the solvent, resulting in droplet fission into smaller droplets. This process repeats as solvent evaporation continues until the solvent is exhausted, eventually producing gas-phase ions of solution species. There are several competing theories regarding the exact mechanism by which these solution species acquire charge, which is proposed to differ with the properties of the analyte molecule.³ The difficulty in studying the electrospray desolvation and ionization process arises in part from the complexity of droplet evolution during the process of solvent evaporation, as

well as the difficulty of detecting the very small amount of charge expected from electrosprayed droplets. Individual ions and clusters formed by the electrospray process have been studied with neutralizer-activated condensation particle growth, 4,5 and other electrode-based techniques using image currents have also been studied for measuring individual ESI droplet charges. However, these aforementioned techniques require very specialized hardware to perform. Thus, techniques capable of simple and accurate ESI droplet charge detection remain scarce. This work explores the effectiveness of a newly developed method to study electrosprayed droplets. This technique has allowed for the direct measurement of charge on electrosprayed droplets without the need for highly specialized equipment.

Electrosprayed droplets meet the definition of an aerosol as they typically have diameters of less than 10 μ m and are suspended in air. As ESI droplets are extremely dynamic and short-lived, traditional off-line aerosol analysis methods such as filter capture are ineffective at exploring the nuances of the charge dynamics of such droplets. Further, typical online

Received: November 29, 2022 Accepted: November 30, 2022 Published: January 11, 2023





techniques such as low-temperature plasma¹⁰ or glow-discharge¹¹ ionization techniques or aerosol mass spectrometers (which typically ablate aerosols with heat¹²) are explicitly designed to ionize species within the aerosols and are therefore unsuitable for study of the initial charge of aerosol droplets produced by ESI. Previous work studying the charge of ESI droplets using printed circuit board (PCB) electrodes has been reported,⁶ as well as experiments indirectly measuring positive charges in droplets via proton activity with pH-sensitive dyes.¹³ However, simple and widely applicable techniques capable of measuring droplet charges are few.

Here we detail a new analytical technique for making such determinations, a novel application of particle into liquid sampling for nanoliter electrochemical reactions (PILSNER). PILSNER was used to measure droplet charges using a unique circuit design, including an electrochemical cell (discussed further in the main text). In PILSNER, an ultramicroelectrode is inserted into a small (nanoliter to low microliter) "collector" droplet situated on a conductive glassy carbon stage which serves as a counter and quasi-reference electrode. Electrochemical techniques are then performed on the contents of the collector droplet directly in real-time, allowing for the sensitive detection of the contents of aerosol particles which were directed at the collector. The basic setups for PILSNER for analyzing electrosprayed droplets are shown and described in Figure 1. In addition to online charge analyses, PILSNER can

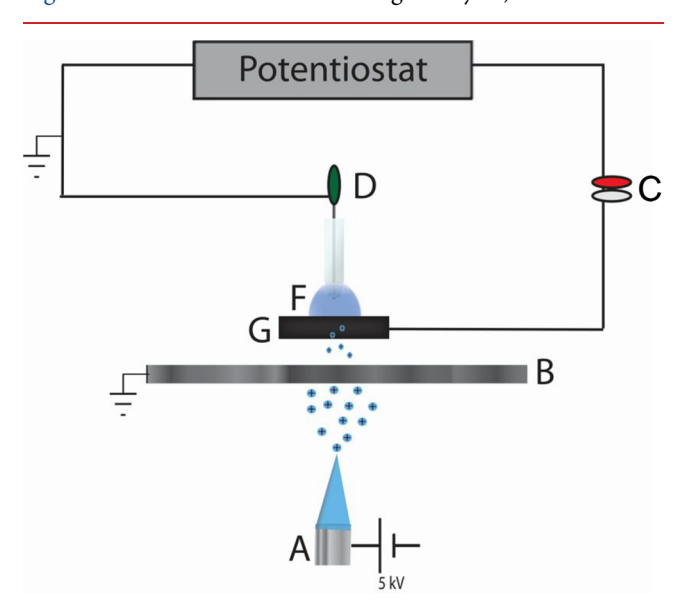


Figure 1. Simplified diagram of PILSNER-ESI. Electrospray is achieved by spraying solution from a capillary (A) against a 70% transparent steel mesh (B) by applying a high (5 kV) voltage difference. (C) and (D) correspond to counter/reference electrode (red/gray) leads, and (D) corresponds to the working electrode (green) lead, respectively. A Pt ultramicroelectrode serves as the working electrode, which is inserted into a water collector droplet (F) atop a glassy carbon stage (G) which serves as the counter/pseudoreference electrode.

electroanalyze the contents of electrosprayed droplets offline and can provide additional information about the solution-phase behavior of charged species from ESI. In this work, PILSNER has been applied to the detection of electrosprayed droplets using open-circuit potential (OCP) and amperometric measurements. These interpretations of the charge deposited

by ESI droplets represent new techniques by which the properties of electrosprayed droplets may be explored.

■ MATERIALS AND METHODS

Materials. The electrode used throughout this work for PILSNER experiments was a platinum scanning electrochemical microscopy tip (10 μ m diameter, R/G ~ 25 based on captured images) obtained from CH Instruments (Austin, TX). The electrode was manipulated using a micropositioner (Model ROE-200, Sutter Instruments) such that the electrode tip was centered within the collector droplet. The glassy carbon quasi-reference/counter electrode was obtained from Alfa Aesar. Solutions and water droplets were prepared with ultrapure water (Millipore Milli-Q, 18.2 MΩ·cm). The solvent used for ESI was a 50:50 mixture of ultrapure water and methanol (Fisher Scientific, Optima grade) to mimic a typical solvent system used in ESI applications. Adventitious ions in solution were found to be sufficient to produce stable electrospray, and no additional solution additives (such as acid) were necessary. The collector droplet for PILSNER consisted of a 10 µL droplet of ultrapure water pipetted onto the glassy carbon surface, except for the experiments concerning droplet viscosity, in which the collector droplet consisted of ultrapure water and 10%, 50%, or 100% glycerol (Sigma-Aldrich, >99%). All experiments were performed within a grounded Faraday cage. The ESI emitter used was a Bruker AP1 stainless steel emitter with a 100 μ m inner capillary diameter, with air as the nebulizing gas supplied at 5 PSI. Voltage during ESI experiments was supplied to the electrically isolated emitter tip with a Spellman model CZE1000R power supply at 5 kV.

PILSNER-ESI with OCP and Amperometry. OCP measurements were performed with a maximum run time of 600 s, a sample interval of 0.005 s (the minimum sampling time achievable with the device), and voltage thresholds of ±1.5 V. Measurements were performed on the CHI model 601D or 6012D potentiostat. All amperometry experiments throughout this work were performed at a sensitivity of 10⁻⁸ A/V (this parameter is not modifiable for OCP experiments). For PILSNER experiments, this resulted in a noise level of \sim 10 pA. Potentiometry was performed with a ~30 s delay before electrospray was introduced in order to establish a stable baseline, as the collector droplets did not contain electrolyte or a strongly poising redox couple. ESI was performed with 50:50 methanol/water solutions introduced at 200 μ L/h using a Cole-Parmer 74800-05 syringe pump and Hamilton gastight 750N 500 µL syringe and PEEK fittings. Electrospray was performed using a potential of 5 kV at a distance of ~1 cm against either a grounded stainless-steel mesh (Figure S1) directly in front of the collector droplet or a grounded steel plate with a circular 150 μ m aperture (referred to throughout as the "steel plate aperture") (Figure S2), as described in each experiment individually, based on the desired frequency of particle interactions with the collector droplet. The purpose of the steel plate aperture was to limit the number of particles reaching the collector droplet; on the contrary, steel mesh (6.3 wires/cm, 0.5 mm diameter wire; transparency of \sim 70%) was used to provide a ground against which to perform ESI, but without significantly inhibiting droplet travel to the collector droplet. ESI experiments were performed with the nebulizing gas and voltage on throughout, with the syringe pump being turned on or off to begin and end each ESI on/off cycle. For experiments involving grounding the quasi-reference electrode,

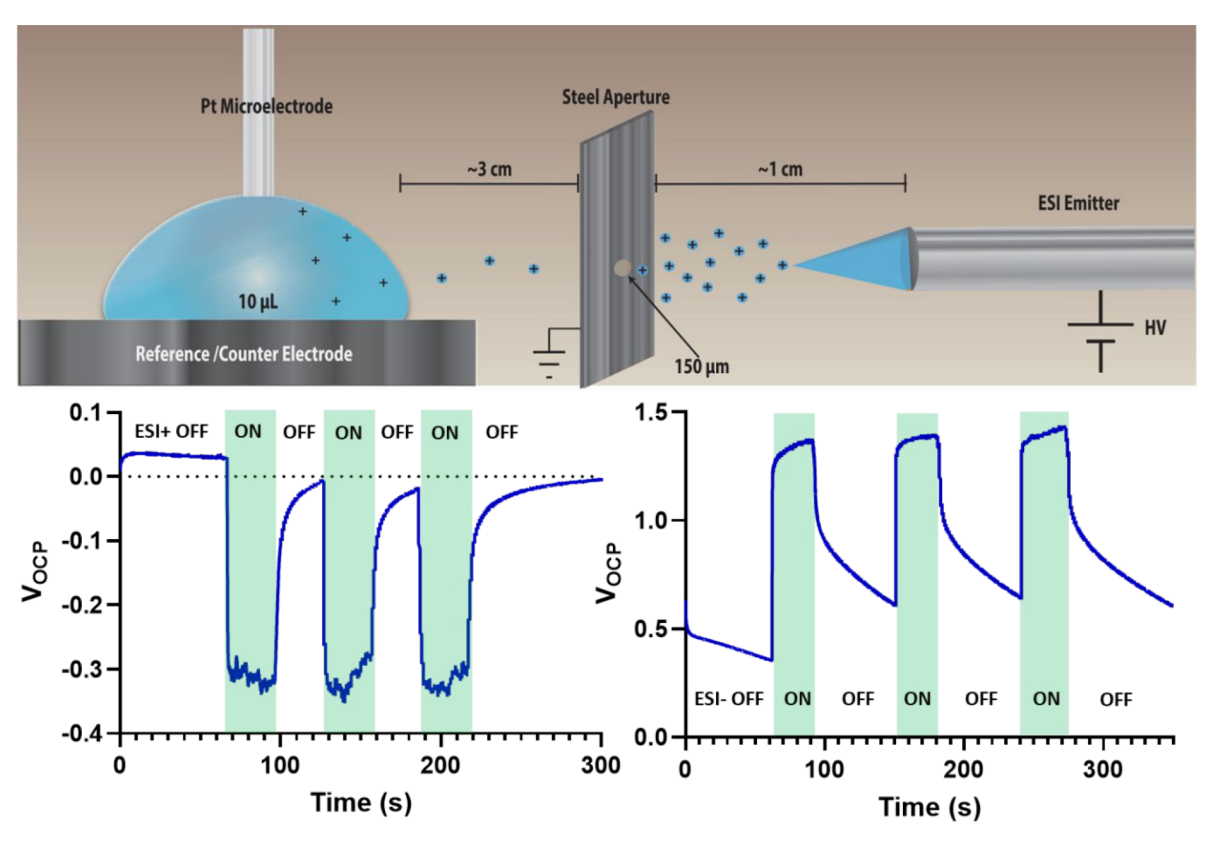


Figure 2. (Top) Diagram of the basic setup for the study of ESI droplets using PILSNER. Droplets are electrosprayed against a grounded aperture using a high voltage (5 kV). Particles which pass through the aperture are detected as they collide with the collector droplet, as described in the text. Diagram not to scale. (Bottom) OCP measurements of exposures of a 10 μ L collector droplet to ESI+ (bottom left) and ESI– (bottom right). Each exposure start and end is indicated by the shaded areas and labels. Exposures were made using the 150 μ m steel plate aperture at a distance of 1 cm.

a chassis ground was manually connected to the stage for ~ 1 s and removed immediately after. Amperometry experiments were run with a constant voltage of 0 V based on a control CV of the collector droplet with a sampling rate of 2 kHz (the maximum sampling rate achievable with the device). To measure exclusively charge being detected on the collector droplet versus on the stage, the stage and collector, respectively, were covered with insulating plastic covers during open-circuit potential experiments while the electrospray was cycled on and off.

Droplet Count and Size Distribution Measurements.

Droplet count and distribution data used to generate estimates of droplet charges were collected using a Grimm model 11-D optical particle counter (31 equidistant channels, size range 253 nm to 35 μ m). The device performs phase Doppler anemometry using a laser to determine aggregate particle sizes and counts using scattered light. Electrospray droplet counts were measured using the same mesh and at the same distance as listed above for the PILSNER experiments, with spray aimed directly at the sampling inlet of the device. The data displayed in Figure 8 are cut off at 8 μ m, as no particles were detected in any experiment or control in the size range of $8-35~\mu m$. Notably, optical aerosol counters tend to exhibit losses and undercounting for aerosol particles at the extreme low end of particle diameters. It is not believed that this probable undercounting had a significant impact on the estimates and calculations detailed in this work, as particles of these sizes contribute extremely little volume to the overall volume of the

droplet population, and the estimates in Figures 8 and S3 are based directly on the volume of collected droplets.

RESULTS AND DISCUSSION

Electrode Response in PILSNER-ESI and Effect of Collector Droplet Viscosity on Steady-State Voltage. The use of PILSNER for the analysis of electrosprayed droplets is shown in Figure 2, top. PILSNER-ESI using OCP produces a large voltage response which is shown in Figure 2, bottom left (ESI+), and Figure 2, bottom right (ESI-). Typically, when interpreting voltages measured during OCP when there is no well-behaved redox pair present, mixedpotential theory is applied to describe the effects of chemical potentials on the measured voltage. In a droplet nominally containing entirely water, a small amount of organic solvent, and the ions expected during ESI such as hydronium ions (ESI +) or water-generated anions such as OH⁻ (ESI-), 15 the OCP voltage (V_{OCP}) would be expected to be determined by mixedpotential theory based on solution-phase species such as H₂O, O2, H+, and OH-. However, in PILSNER-ESI, a large and immediate voltage shift is observed in both ESI+ and ESI-(Figure 2). These voltage shifts exceed what would be expected for changing concentrations of solution-phase species in the collector droplet. To explain these results, alternate mechanistic hypotheses to mixed-potential theory must be considered. Specifically, voltages and currents in PILSNER-ESI are interpreted as induced charges from deposited droplets leading directly to current flow in the system. These current

flows can then be interpreted with amperometry or OCP to detect droplet charges.

When ESI is off during PILSNER-ESI, the baseline is quasistable due to a lack of redox pair capable of poising the potential of the system. When ESI+ begins, the $V_{\rm OCP}$ drops rapidly until it reaches a quasi-steady-state voltage. Once the spray is turned off, the signal decays rapidly for a short duration (seconds) and then decays more slowly over a longer duration (tens of seconds). This process does not modify the droplet permanently, and multiple on/off cycles can be performed on the same collector droplet so long as it has not evaporated. Additionally, the direction of the voltage shift is initially counterintuitive (negative voltage in ESI+ and vice versa). These phenomena cannot be reasonably explained with chemical potential arguments regarding the addition of H+ or OH to the collector droplet by the electrospray. Using a chemical potential explanation, the large voltage changes observed (on the order of 0.5-1.5 V) would correspond to immediate collector droplet pH changes of approximately 8 to 25 based on the Nernst equation. Normally, a roughly ± 59 mV shift in $V_{\rm OCP}$ per 10-fold change in the reaction quotient of [H⁺]/[OH⁻] would be expected. The experimental result in Figure 2 is thus both physically unrealistic as well as in sharp disagreement with other research which has indicated that the pH change that occurs in droplets produced via ESI+ is at most around 2-3 pH units. ^{13,16} A hypothesis for these observations is detailed below and in Figure 3. Rather than

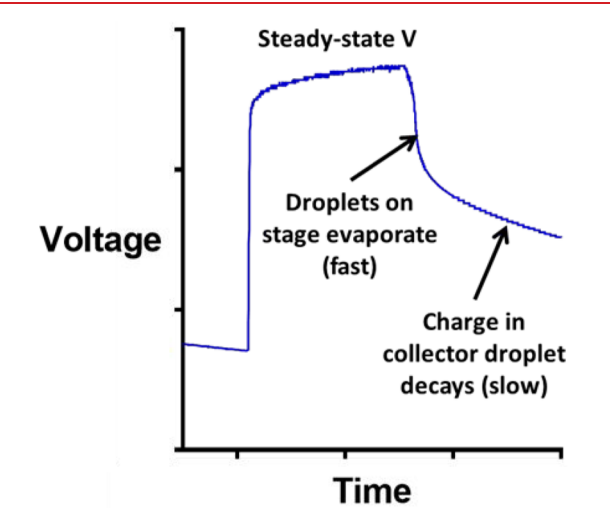


Figure 3. Zoom-in of an on/off cycle of an ESI— exposure using PILSNER. We hypothesize that, once the electrospray is turned off, a rapid evaporation and decay of charged droplets collected on the stage (counter/quasi-reference electrode) causes a fast drop in measured voltage, followed by a slower decay of the charge remaining in the collector droplet.

reading a traditional chemical potential, the working electrode in the case of PILSNER-ESI is actually directly measuring accumulated charge which has deposited via the electrosprayed droplets either into the collector droplet or onto the glass carbon stage. This unbalanced charge is likely relieved by the donation or acceptance of electrons at the electrode surfaces to or from solution species.

Through a similar mechanism, aggregate current transients induced by collected droplets can be observed during PILSNER-ESI with an amperometry measurement, an example of which is shown in Figure 4. The bidirectional currents

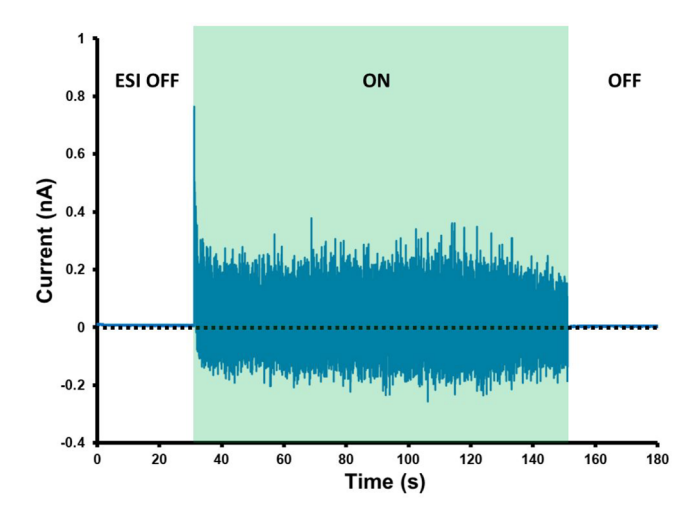


Figure 4. Amperometry experiment of ESI+ of water sprayed into a 10 μ L water collector droplet through the 150 μ m steel aperture (0 V applied, sampling rate 1 kHz, ESI+ on at t=40s and off at t=120 s). The fluctuations in current are believed to be summations of many individual current events occurring as droplets land on the collector and stage.

observed during ESI+ exposure are expected, as it has been reported that both positive and negatively charged droplets are formed during both ESI+ and ESI-, though the majority of droplets match the polarity of the applied voltage.⁶⁻⁸

As a consequence of its greater surface area, the stage is subjected to a greater amount of the charge compared to the working electrode, causing the voltage at the reference electrode to rise relative to ground. This rise is interpreted as a drop in the working electrode potential when measuring $V_{\rm OCP}$, as the displayed voltage is relative to the reference, which is normally assumed to be constant. The direction of $V_{\rm OCP}$ in PILSNER-ESI is therefore "flipped" (positively charged droplets produce a negative change in $V_{\rm OCP}$ and vice versa). As charge continuously deposits into the collector droplet and onto the stage, a steady-state or limiting $V_{\rm OCP}$ is reached when the rate of charge deposition matches the rate of dissipation caused by donation (or extraction) of electrons at the working electrodes and/or evaporation of collected droplets. When the ESI is turned off, any charge from the small droplets that were depositing onto the surface of the stage and potentially contributing to the charge of the reference electrode is rapidly donated, causing a fast dip in the voltage magnitude, but charge remaining in the collector droplet is not immediately dissipated and decays more slowly, resulting in the seemingly two-stage $V_{\rm OCP}$ decay curves that were observed. This hypothesis regarding the location of charge deposition is supported by the data shown in Figure 5. In Figure 5, the ESI-PILSNER collection setup has been altered to have either the stage (counter/reference electrode) or the working electrode and collector droplet covered with insulating plastic to prevent electrosprayed droplet interaction with the collector or stage. Notably, in the "droplet and electrode blocked" configuration, the collector droplet is insulated from electrosprayed droplets landing in the collector itself, but the collector droplet is still in contact with the stage. As a result, charge events occurring on the stage may still produce a detectable current. The $V_{\rm OCP}$ responses observed indicate that a majority of the charge detection occurs on the stage and a minority occurs in the collector droplet. Droplets which land on the stage are still

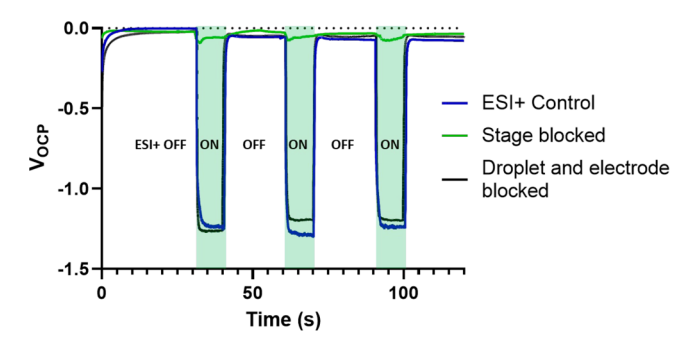


Figure 5. $V_{\rm OCP}$ responses during ESI+ to the counter/reference electrode stage (green) or the 10 $\mu \rm L$ water collector droplet and working electrode (black) being covered and electrically insulated versus a control experiment (blue). Voltages shown are normalized to a starting $V_{\rm OCP}$ of 0 V. The PILSNER system was exposed to 200 $\mu \rm L/h$ ESI+ for 10 s intervals starting at 30, 60, and 90 s.

electrically connected to the working electrode via the collector, and thus, charge elimination mechanisms are expected to be similar to those in the collector droplet (discussed further below).

The rate of charge decay in the collector droplet, by this hypothesis, is affected directly by the viscosity of the collector droplet and how quickly charged species can move through the droplet to be sensed at the electrodes. The limiting V_{OCP} is also directly linked to viscosity of the collector droplet. This is supported by the fact that, under identical conditions such as in Figure 2, the $V_{\rm OCP}$ magnitude observed for ESI+ is much smaller than in ESI- by a factor of roughly 2-3 (protons diffuse through water very rapidly through Grotthuss shuttling,¹⁷ whereas anions do not). This hypothesis was also tested by performing PILSNER-ESI on collector droplets consisting of varying fractions of glycerol and water to artificially change the collector viscosity (representative traces shown in Figure 6). It was found that, for both positive and negative mode ESI, a high fraction of glycerol resulted in significant increases to the magnitude of $V_{\rm OCP}$, consistent with a slower rate of charge diffusion to the working electrode (n =3). These results strongly indicate that PILSNER, in addition to its ability to perform electrochemical measurements on electrically neutral solutions, also has the ability to directly detect charged species using a novel direct-detection method not usually utilized with ultramicroelectrodes.

Effect of Grounding on Charge Decay. It was also hypothesized that, based on the species previously reported during ESI+ (mostly hydronium) and ESI- (mostly radical anions and OH⁻), ¹⁸ the mechanism of charge elimination at the working electrode could be kinetically examined in the PILSNER collector droplet. The most thermodynamically simple mechanism of unbalanced proton or hydronium ion resolution would be

$$2H^{+}(aq) + 2e^{-} \rightarrow H_{2}(g)$$
 (1)

Here, the electrons are supplied by one of the electrodes. This process is bimolecular and would likely have a significant rate-limiting step of proton combination. By comparison, a radical anion or OH- species would theoretically be able to directly donate excess electrons directly and quickly to a ground or through an electrode, if such a thermodynamically favorable path were available. By this reasoning, charge elimination in the collector droplet would occur either at the working or counter electrode, while droplets landing on the stage would eliminate charge to the counter electrode exclusively. To test this hypothesis regarding charge elimination, experiments were performed where a path to chassis ground was introduced for 1 s at the same time the spray was turned off during ESI+ and ESI- on/off cycling. The data for these experiments are shown in Figure 7. Each red asterisk represents the introduction of a 1 s ground (the first on/off cycle was not grounded for comparison purposes). During ESI + and ESI- experiments, grounding the stage upon ESI cessation briefly causes the measured voltage to go to 0 V, which is expected, since the introduction of a ground completes the open circuit being measured and sets the working electrode potential equal to the chassis ground. However, different responses postground are observed for positive and negative mode experiments. Compared to the first on/off cycle (control), the ESI+ experiment shows that the voltage postground rebounds rapidly and follows nearly the exact same decay curve as the control. This is consistent with the grounding event being ineffective at removing much charge, which is consistent with a slower migration process which cannot immediately vacate charge into the ground. In an opposite fashion, the ESI- experiment shows a significant difference between the control and grounded cycles. Once grounded, the negative mode voltage decay curve is permanently altered and shows a substantially diminished $V_{
m OCP}$ magnitude compared to the control curve. This is

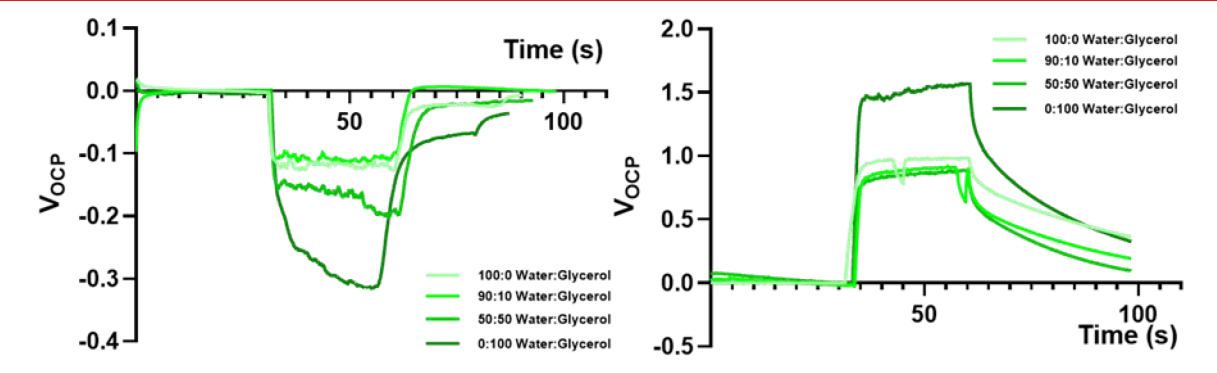


Figure 6. PILSNER-ESI OCP baseline-corrected plots of 30 s ESI+ (left) and ESI– (right) exposures of 0, 10, 50, and 100% glycerol collector droplets, adjusted to the same starting voltage. $V_{\rm OCP}$ at steady state was determined from the difference in the magnitude of $V_{\rm OCP}$ for the 30 s exposure and the average V 10 s prior to the beginning of spray. A significant increase in $V_{\rm OCP}$ magnitude was observed at high glycerol fractions. Both experiments utilized the 150 μ m steel plate aperture.

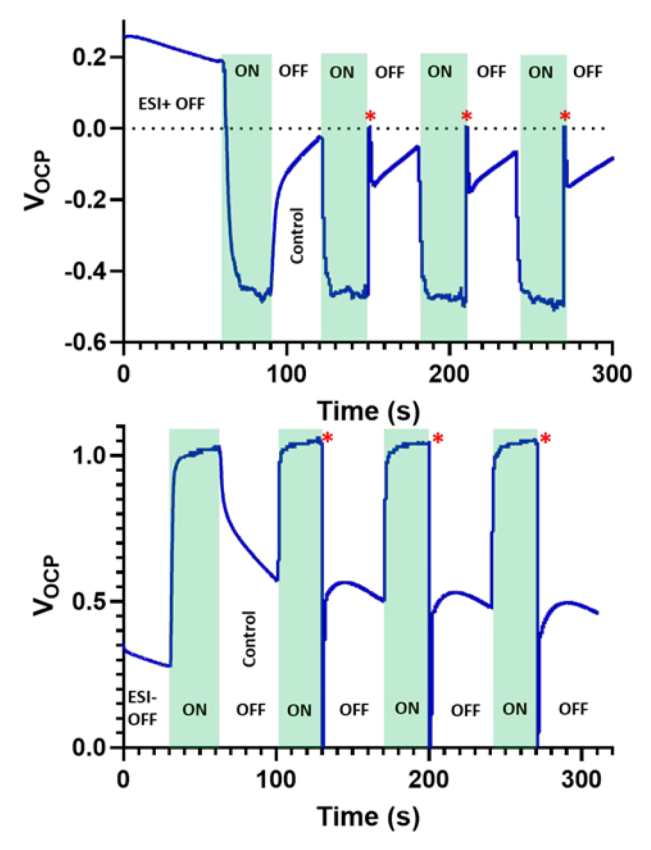


Figure 7. ESI+ (top) and ESI– (bottom) experiments using the 150 $\mu \rm m$ steel plate aperture in which the spray was cycled on and off, but a chassis ground was briefly applied for 1 s at the last three of four on/ off cycles (red asterisk). Note the differences in $V_{\rm OCP}$ decay curve shape between ESI+ and ESI– postgrounding.

hypothesized to be indicative of a faster charge elimination mechanism as described previously. This suggests that PILSNER is capable of qualitatively measuring the relative diffusivity and mobility of charged species in solution in the collector droplet.

Estimation of Droplet Charges via Fluorescein Proxy. Determining the charge on individual droplets collected during PILSNER-ESI is challenging, in large part due to the difficulty of directly determining the number and size of particles being

collected on the stage and collector droplet per unit time. To determine the average number of charges per electrosprayed droplet, two solutions of different concentrations of fluorescein (2 and 20 mM) in water were electrosprayed at the PILSNER-ESI setup while an amperometric measurement applying 0 V was being made. The total charge collected during these amperometry experiments was integrated to determine the total amount of charge and from that the number of fundamental charges, collected during each 30 s experiment. The fluorescein that deposited on the stage during these experiments was then used as a tracer in the determination of how many droplets were actually collected. Fluorescein was extracted from the stage and electrode by serial rinsing with the same 1 mL volume of water. The amount of fluorescein in the extract was measured via a separate calibration (example in Figure 8, left plot) by fluorescence emission under a microscope. By estimating that the concentration of fluorescein in the electrosprayed droplets was constant at 2 or 20 mM, and by accounting for the dilution made upon extraction from the stage, the total volume of droplets collected onto the stage over the course of the 30 s amperometry experiment could be determined. To determine particle size distributions, an optical counter was used to measure aerosol counts as a function of droplet diameter (example in Figure 8, right plot). The total number of fundamental charges calculated previously was then divided by the sum of these bin counts to produce an average number of charges per droplet. The calculated average number of charges per droplet for the 20 mM (n = 3) and 2 mM (n =3) fluorescein solutions were 178 \pm 14 and 379 \pm 119 charges, respectively. More detailed plots of calculated droplet charges as a function of droplet diameter for these data are shown and discussed in Figure S3. These numbers are reasonable given that the previously cited number of a few thousand charges per ESI droplet⁶ refer to droplets immediately following generation. The droplets collected in these experiments would likely have undergone some degree of evaporation and fission en route to the PILSNER stage, reducing their average charges per droplet. Furthermore, an important assumption in the above calculation is that all of the fluorescein extracted from the stage was derived from charged droplets. It is likely that some fraction of the droplets generated by ESI consisted of neutrals, 19 thus contributing to the observed number of droplets without actually contributing to the

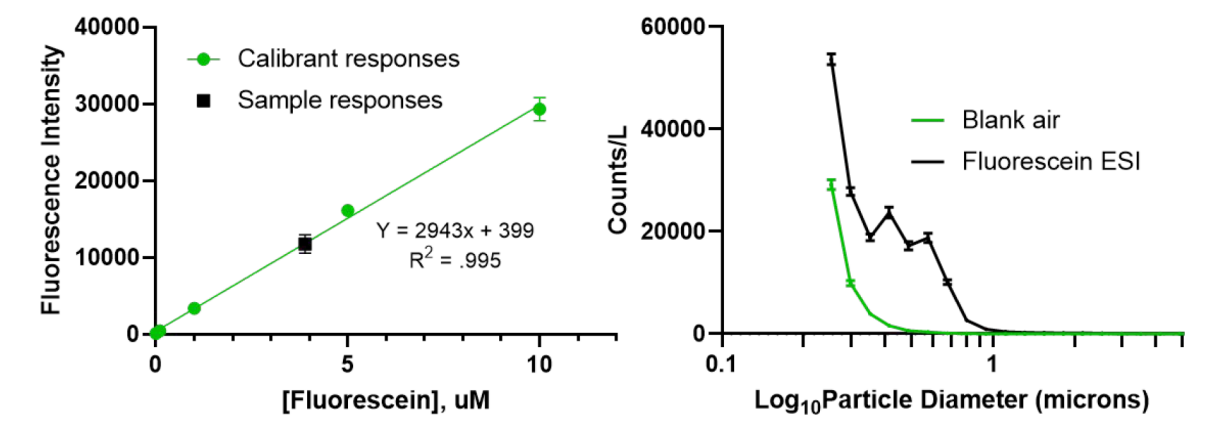


Figure 8. (Left) Example fluorescence calibration curve, as measured by emission spectroscopy (excitation: 490 nm, emission: 510 nm), used in the determination of the total amount of fluorescein collected during the 20 mM fluorescein ESI exposure experiment outlined in the main text. Black inset indicates the extract sample measurements (n = 3). (Right) Example particle size distribution of electrosprayed droplets of 20 mM fluorescein in water, as measured by a Grimm 11-D optical counter (n = 3). The data for the 2 mM fluorescein trial are shown in Figure S4.

amount of charge measured from the amperogram. This would cause a skew toward a smaller number of calculated charges per droplet. This calculation is also limited by the maximum sampling rate of the potentiostat (\sim 2 kHz), which limits the accuracy of the charge integration calculation.

CONCLUSION

We demonstrate the applicability of particle-into-liquid sampling for nanoliter electrochemical reactions (PILSNER) to the study of the properties of electrosprayed droplets using open circuit potential (V_{OCP}) . Data-driven hypotheses regarding collector droplet dynamics and the mechanism of charge detection in PILSNER-ESI are presented, as well as data indicating that the diffusivity of species in the collector droplet affects the voltage response observed during PILSNER-ESI. The behavior of the system also suggests that the mechanism of charge elimination at the working electrode surface is affected by the mode of electrospray. Amperometric measurement during PILSNER-ESI of a fluorescent tracer is also shown as a method of directly calculating the aggregate charge of electrosprayed droplets. These measurement capabilities demonstrate that PILSNER is a viable and simple tool for the measurement of the charge properties of droplets and aerosols.

ASSOCIATED CONTENT

Supporting Information

The Supporting Information is available free of charge at https://pubs.acs.org/doi/10.1021/jasms.2c00338.

PILSNER setups, post of ESI droplet charges, and fluorescein ESI calibration curve (PDF)

AUTHOR INFORMATION

Corresponding Author

Jeffrey E. Dick — Department of Chemistry, The University of North Carolina at Chapel Hill, Chapel Hill, North Carolina 27599, United States; Lineberger Comprehensive Cancer Center, School of Medicine, The University of North Carolina at Chapel Hill, Chapel Hill, North Carolina 27599, United States; orcid.org/0000-0002-4538-9705; Email: jedick@email.unc.edu

Authors

Nathaneal A. Park – Department of Chemistry, The University of North Carolina at Chapel Hill, Chapel Hill, North Carolina 27599, United States

Gary L. Glish – Department of Chemistry, The University of North Carolina at Chapel Hill, Chapel Hill, North Carolina 27599, United States; Occid.org/0000-0003-2418-4126

Complete contact information is available at: https://pubs.acs.org/10.1021/jasms.2c00338

Notes

The authors declare no competing financial interest.

ACKNOWLEDGMENTS

The authors would like to thank Nicole L. Walker, Collin J. McKinney, Kathryn J. Vannoy, and Thomas B. Clarke for insightful discussions, edits, and help with the preparation of graphics. This work was completed with financial support from the Chemical Measurement and Imaging Program in the National Science Foundation Division of Chemistry under

Grant CHE-2003587 and the Sloan Foundation (FG-2021-15486). This work was supported by the U.S. Army Engineer Research and Development Center (ERDC), Installations and Operational Environments (IOE) Program under Contract number W912HZ2120055. Use of trade, product, or firm names in this manuscript is for descriptive purposes only and does not imply endorsement by the U.S. Government. The content of this work is the sole responsibility of the authors, and does not necessarily reflect the views of the aforementioned contributing funding organizations.

REFERENCES

- (1) Yamashita, M.; Fenn, J. B. Electrospray Ion Source. Another Variation of the Free-Jet Theme. *J. Phys. Chem.* **1984**, *88*, 4451–4459.
- (2) Rohner, T. C.; Lion, N.; Girault, H. H. Electrochemical and Theoretical Aspects of Electrospray Ionisation. *Phys. Chem. Chem. Phys.* **2004**, *6*, 3056–3068.
- (3) Konermann, L.; Ahadi, E.; Rodriguez, A. D.; Vahidi, S. Unraveling the Mechanism of Electrospray Ionization. *Anal. Chem.* **2013**, 85 (1), 2–9.
- (4) Rosell-Llompart, J.; Loscertales, I. G.; Bingham, D.; Fernández de la Mora, J. Sizing Nanoparticles and Ions with a Short Differential Mobility Analyzer. *J. Aerosol Sci.* **1996**, 27 (5), 695–719.
- (5) Gamero-Castaño, M.; de la Mora, J. F. A CONDENSATION NUCLEUS COUNTER (CNC) SENSITIVE TO SINGLY CHARGED SUB-NANOMETER PARTICLES. J. Aerosol Sci. 2000, 31 (7), 757–772.
- (6) Gao, J.; Austin, D. E. Mechanistic Investigation of Charge Separation in Electrospray Ionization Using Microparticles to Record Droplet Charge State. J. Am. Soc. Mass Spectrom. 2020, 31, 2044.
- (7) Zilch, L. W.; Maze, J. T.; Smith, J. W.; Ewing, G. E.; Jarrold, M. F. Charge Separation in the Aerodynamic Breakup of Micrometer-Sized Water Droplets. *J. Phys. Chem. A* **2008**, *112* (51), 13352–13363
- (8) Maze, J. T.; Jones, T. C.; Jarrold, M. F. Negative Droplets from Positive Electrospray. *J. Phys. Chem. A* **2006**, *110* (46), 12607–12612.
- (9) Kaiser, J. Mounting Evidence Indicates Fine-Particle Pollution. Science 2005, 307 (5717), 1858–1861.
- (10) Spencer, S. E.; Tyler, C. A.; Tolocka, M. P.; Glish, G. L. Low-Temperature Plasma Ionization-Mass Spectrometry for the Analysis of Compounds in Organic Aerosol Particles. *Anal. Chem.* **2015**, *87* (4), 2249–2254.
- (11) Dalton, C. N.; Jaoui, M.; Kamens, R. M.; Glish, G. L. Continuous Real-Time Analysis of Products from the Reaction of Some Monoterpenes with Ozone Using Atmospheric Sampling Glow Discharge Ionization Coupled to a Quadrupole Ion Trap Mass Spectrometer. *Anal. Chem.* **2005**, *77* (10), 3156–3163.
- (12) Canagaratna, M. R.; Jayne, J. T.; Jimenez, J. L.; Allan, J. D.; Alfarra, M. R.; Zhang, Q.; Onasch, T. B.; Drewnick, F.; Coe, H.; Middlebrook, A.; Delia, A.; Williams, L. R.; Trimborn, A. M.; Northway, M. J.; DeCarlo, P. F.; Kolb, C. E.; Davidovits, P.; Worsnop, D. R. Chemical and Microphysical Characterization of Ambient Aerosols with the Aerodyne Aerosol Mass Spectrometer. *Mass Spectrom Rev.* 2007, 26 (2), 185–222.
- (13) Van Berkel, G. J.; Zhou, F.; Aronson, J. T. Changes in Bulk Solution PH Caused by the Inherent Controlled-Current Electrolytic Process of an Electrospray Ion Source. *Int. J. Mass Spectrom Ion Process* 1997, 162 (1–3), 55–67.
- (14) Kauffmann, P. J.; Park, N. A.; Clark, R. B.; Glish, G. L.; Dick, J. E. Aerosol Electroanalysis by PILSNER: Particle-into-Liquid Sampling for Nanoliter Electrochemical Reactions. *ACS Measurement Science Au* **2022**, *2*, 106.
- (15) Kebarle, P.; Verkerk, U. H. Electrospray: From Ions in Solution to Ions in the Gas Phase, What We Know Now. *Mass Spectrom Rev.* **2009**, 28 (6), 898–917.
- (16) Liigand, P.; Heering (Suu), A.; Kaupmees, K.; Leito, I.; Girod, M.; Antoine, R.; Kruve, A. The Evolution of Electrospray Generated

Droplets Is Not Affected by Ionization Mode. J. Am. Soc. Mass Spectrom. 2017, 28 (10), 2124-2131.

- (17) Knight, C.; Voth, G. A. The Curious Case of the Hydrated Proton. Acc. Chem. Res. 2012, 45 (1), 101-109.
- (18) van Berkel, G. J.; Kertesz, V. Using the Electrochemistry of the Electrospray Ion Source. Anal. Chem. 2007, 79 (15), 5510-5520.
- (19) Jaworek, A.; Gañán-Calvo, A. M.; Machala, Z. Low Temperature Plasmas and Electrosprays. J. Phys. D Appl. Phys. 2019, 52 (23), 233001.

Recommended by ACS

A High Kinetic Energy Ion Mobility Spectrometer for Operation at Higher Pressures of up to 60 mbar

Florian Schlottmann, Stefan Zimmermann, et al.

MARCH 31, 2023

JOURNAL OF THE AMERICAN SOCIETY FOR MASS SPECTROMETRY

READ **'**

Analysis of Liquid Particles in Aerosols via Charge-Induction Amperometry (ALPACA) for Rapid Electrospray Droplet **Charge Analysis**

Nathaneal A. Park, Jeffrey E. Dick, et al.

JANUARY 11, 2023

JOURNAL OF THE AMERICAN SOCIETY FOR MASS SPECTROMETRY

READ 🗹

Development of a Structure for Lossless Ion Manipulations (SLIM) High Charge Capacity Array of Traps

Adam P. Huntley, Yehia M. Ibrahim, et al.

FEBRUARY 23, 2023

ANALYTICAL CHEMISTRY

READ 🗹

Experimental Validation of the Digital Tandem Mass Filter

Fatima Olayemi Obe, Peter T. A. Reilly, et al.

JANUARY 09, 2023

JOURNAL OF THE AMERICAN SOCIETY FOR MASS SPECTROMETRY

READ **'**

Get More Suggestions >